IOP Conf. Series: Materials Science and Engineering **418** (2018) 012052 doi:10.1088/1757-899X/418/1/012052

Experimental Investigation of Forming Limit Curve for AA5754-O

W N Yuan[1], M Wan[1] and X D Wu[1]

[1] School of Mechanical Engineering and Automation, Beihang University, Beijing, 100191, P.R. China

E-mail: nicestnan@sina.com

Abstract. The Forming Limit Curve (FLC) is a line that is consisted of the major and minor strain pairs for different kinds of strain paths. It is widely adopted for the quantitative description of the sheet metal formability. In this paper, a stand-alone servo-motor apparatus associated with the high-accuracy measurement system was developed, based on which the FLC of AA5754-O with the thickness of 3.0mm was investigated. Firstly, the material properties of metal sheet were explored and the anisotropic coefficients in the constitutive law were calculated to describe the yield behaviour. Secondly, in order to increase the strain level of cruciform specimens, various simulations with different shapes of specimens were performed with ABAQUS/Explicit. Finally, the biaxial tensile tests with the optimized shape of cruciform specimens were performed under different loading ratio conditions. The experimental FLC of AA5754-O was obtained. The fracture zone of each specimen was occurred in the central region without premature arm fracture, which verified the feasibility of the cruciform specimen purposed.

1. Introduction

Sheet metal forming technology plays a very important role in the manufacturing industry and is intensively used in the fields of automobile, aviation, aerospace, electronics and so on. Generally, the forming limit could be separated into the forming limit stress and the forming limit strain, which could be converted to each other based on the constitutive equation of the sheet metal. In 1946, Handin [1] analyzed the instability evolution of the sheet metal under different strain paths conditions and the concept of limit strain based on the principal strain was firstly proposed. The forming limit curve (FLC) made up of major strain and minor strain is an effective instrument to estimate the capability to undergo plastic deformation to a given shape without any defects [2]. In general, FLC could be obtained via the following approaches.

Analytically, diffuse instability theory and localized instability theory are commonly applied to predict the sheet metal forming limit [3]. The constitutive equations of the materials could be obtained by the uniaxial tensile tests. The yield criterion and hardening law at different proportional loading paths could be realized via biaxial tensile tests, based on which the yield functions and harden models could be established. M-K model proposed by Marciniak and Kuczynski [4] was widely used due to its effectiveness. Bolin Ma et al [5] analyzed the effect of through-thickness normal stress on sheet formability based on M-K model. Baosheng Liu et al [6] made the predicted FLC of 5A90 aluminum alloy by a modified M-K model, which showed a good accordance with the experimental results. However, the process of theoretical prediction is considerable complex.

Content from this work may be used under the terms of the Creative Commons Attribution 3.0 licence. Any further distribution of this work must maintain attribution to the author(s) and the title of the work, journal citation and DOI.
Published under licence by IOP Publishing Ltd

Experimentally, the "in-plane stretching' test and the "out-of-plane stretching" test are two commonly used methods to obtain the FLC of sheet metal. A flat punch and a hemispherical punch were utilized during the process, respectively. Different strain paths were generated by varying the width of the metal sheet. However, owing to the existence of friction between sheet and punch, the deformation behavior was affected in punch stretch tests. Apart from the standard methods, the biaxial tensile test with the cruciform shape specimen was put forward by Institution [7] to determine the forming limit. Zidane et al [8] determined the FLC characterization of metallic sheets by means of in-plane biaxial test. The whole test was immune to any effect of friction and different strain paths could be realized by controlling the loading or displacement of the actuators.

In this study, the stress-strain curves of AA5754-O were obtained through uniaxial tensile tests. Then, a stand-alone servo-motor apparatus associated with the high-accuracy measurement system was developed. The biaxial tensile tests were performed according to the international standard ISO16842-201415 [9], and then the anisotropy parameters of Yld2000-2d yield criterion were calculated, which were used for the optimization simulations of cruciform specimen. Based on the biaxial tensile tests at different loading ratios, the FLC of AA5754-O was finally determined. Meanwhile, the reliability of the cruciform specimen purposed was well verified.

2. Material properties

2.1. Experiments of uniaxial tests

In this study, AA5754-O with the thickness of 3.0mm was used for the formability characterization and its chemical composition was given in table 1.

Table 1. Chemical composition of AA5754-O (wt. %)

Element	Al	Mg	Mn	Fe	Si	Cu	Ni	Ti	Zn
Wt. %	Bal	3.0	0.24	0.26	0.03	0.02	<0.01	<0.01	<0.01

The specimens were manufactured along the rolling direction, the diagonal direction and the transverse direction using ASTM E8 standard specimen. Each direction was duplicated three times and the average values were calculated aiming to improve the accuracy and minimize man-made error. The true stress-strain curves obtained from the tests were plotted in figure 1.

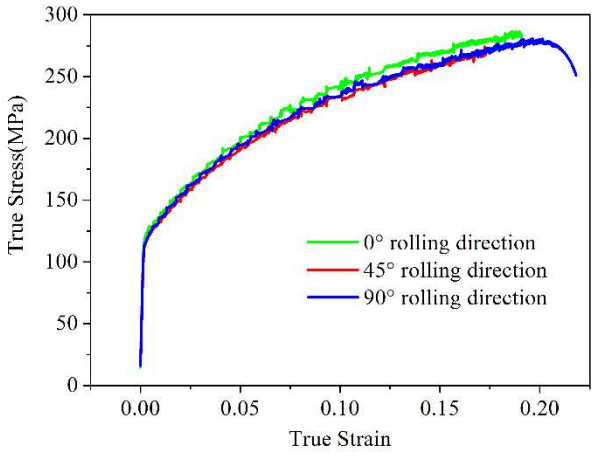


Figure 1. The true strain- true stress curves of AA5754-O.

The true stress-plastic strain data was fitted by Swift hardening law [10], as shown in Eq. (1).

$$\sigma = K(\varepsilon + \varepsilon_0)^n \tag{1}$$

where σ and ε are the plastic stress and the plastic strain respectively, K is the strength constant value, n is the strain hardening exponent, ε_0 is the yield strain. The mechanical properties of the AA5754-O acquired from uniaxial tensile tests and corresponding fitting procedures were listed in table 2. The *r*-value was estimated as $r = \varepsilon_w / \varepsilon_t$, where ε_w was the width strain and ε_t was the thickness strain obtained based on the assumption of volume conservation [11]. Both the strain along the tension direction and the width strain were measured by digital image correlation method.

Table 2. Mechanical properties of AA5754-O from uniaxial tests.

Direction(°)	$\sigma_{0.2}$(MPa)	E (MPa)	n	K (MPa)	r-value
0	125.2	71935.3	0.297	467.73	0.688
45	119.2	66491.9	0.302	457.02	0.777
90	120.1	64673.7	0.285	446.54	0.608

2.2. Experiments of biaxial tests

The biaxial tensile testing system applied in the current study was a stand-alone servo-motor apparatus associated with digital speckle correlation measurement (DSCM) system as shown in figure 2. The servo-motor control has the advantages of lower noise and slighter vibration when compared with servo-hydraulic control. Signal from PLC unit with preprogramed PID closed-loop controlling code was conveyed to the actuators aiming to conduct accurate biaxial tensile test obeying given proportional loading path. The displacement control error in this machine is lower than 0.02mm, which could make it reliable to ensure the centre of the specimen maintains stationary during the test.

DSCM is a practical and effective optical technique for motion and deformation measurement [12]. It possesses the advantages of simple experimental set-up, high precision and high degree of automation and reliability when compared with conventional strain gauge. DSCM has been widely used in many fields. The basic principle of DSCM could be simply described by correlation matching between the same subsets located in the images before and after deformation. The displacement field with sub-pixel precision was calculated, and the strains were subsequently further obtained.

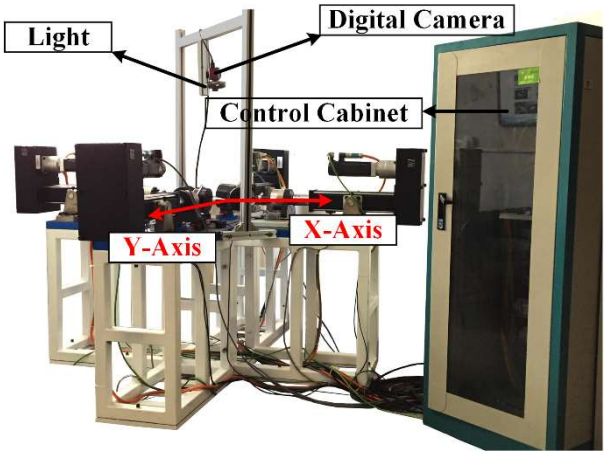


Figure 2. Biaxial tensile apparatus.

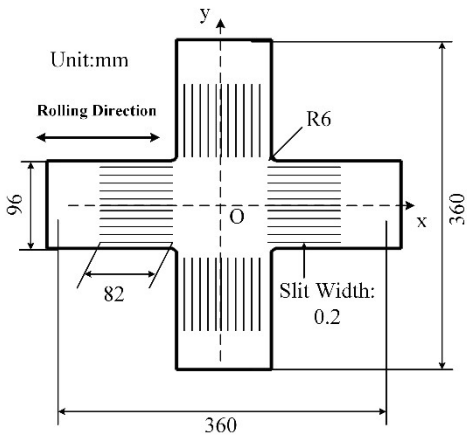


Figure 3. The geometry of cruciform specimen.

According to the international standard proposed in 2014 [9], three cruciform specimens with the geometry shown in figure 3 were performed under the equai-biaxial condition to eliminate the random

error of the experiments. The material properties acquired from biaxial tests and the average values were calculated and listed in table 3.

Table 3. Mechanical properties of AA5754-O from biaxial tests.

Groups	σ_b(MPa)	r_b
1	125.21	1.68
2	124.88	1.35
3	126.05	1.19
Average	125.07	1.41

2.3. Yld2000-2d yield criterion

The Yld2000-2d is a non-quadratic anisotropic yield criterion, which could predict more precisely plastic deformation of the aluminum alloy. Consequently, Yld2000-2d yield function was adopted in this study, and is expressed as the following expression:

$$\phi = \phi' + \phi'' = 2\sigma_e^m \tag{2}$$

Where

$$\begin{cases} \phi' = |Y_1' - Y_2'|^m \\ \phi'' = |2Y_1'' + Y_2''|^m + |2Y_2'' + Y_1''|^m \end{cases} \tag{3}$$

Y_i' and Y_i'' $(i = 1,2)$ are the principle values of the matrices X' and X'':

$$\begin{cases} Y_i' = \frac{1}{2}(X_{11}' + X_{22}' \pm \sqrt{(X_{11}' - X_{22}')^2 + 4X_{12}'^2}) \\ Y_i'' = \frac{1}{2}(X_{11}'' + X_{22}'' \pm \sqrt{(X_{11}'' - X_{22}'')^2 + 4X_{12}''^2}) \end{cases} \tag{4}$$

The components of X' and X'' are acquired by performing linear transformation on Cauchy stress tensor, as shown in Eq. (5)

$$\begin{cases} X' = L'\sigma \\ X'' = L''\sigma \end{cases} \tag{5}$$

Where

$$\begin{bmatrix} L'_{11} \\ L'_{12} \\ L'_{21} \\ L'_{22} \\ L'_{66} \end{bmatrix} = \begin{bmatrix} 2/3 & 0 & 0 \\ -1/3 & 0 & 0 \\ 0 & -1/3 & 0 \\ 0 & 2/3 & 0 \\ 0 & 0 & 1 \end{bmatrix} \begin{bmatrix} \alpha_1 \\ \alpha_2 \\ \alpha_7 \end{bmatrix} \tag{6}$$

$$\begin{bmatrix} L''_{11} \\ L''_{12} \\ L''_{21} \\ L''_{22} \\ L''_{66} \end{bmatrix} = \frac{1}{9} \begin{bmatrix} -2 & 2 & 8 & -2 & 0 \\ 1 & -4 & -4 & 4 & 0 \\ 4 & -4 & -4 & 1 & 0 \\ -2 & 8 & 2 & -2 & 0 \\ 0 & 0 & 0 & 0 & 9 \end{bmatrix} \begin{bmatrix} \alpha_3 \\ \alpha_4 \\ \alpha_5 \\ \alpha_6 \\ \alpha_8 \end{bmatrix} \tag{7}$$

The Cauchy stress tensor σ are the eight anisotropy coefficients α_1-α_8 could be determined by eight input data of sheet metal from uniaxial tension tests along three directions to the rolling direction and

equal-biaxial tension tests. The value of non-quadratic exponent *m* is set to be 8. The parameters are listed in table 4.

Table 4. Anisotropy parameters of Yld2000-2d for AA5754-O.

α_1	α_2	α_3	α_4	α_5	α_6	α_7	α_8
0.9278	1.0329	0.9479	1.0446	1.0091	0.9480	1.0201	1.1509

3. Specimen design

At present, the biaxial tensile test international standard ISO16842-201415 has been established, which is utilized to investigate the yield behavior of the material. However, for this shape of cruciform specimen, the strain level at the central region of specimen is relatively low and the forming limit state could not be reached. Besides, the strength of the slitted arm is low, which could lead the premature arm fracture. As a result, this shape of cruciform specimen was not suitable for the study of the forming limit curve. To characterize the formability of metal, numerous researchers purposed that central thickness reduction of the specimen could be helpful to increase the deformation during the test and decrease the influence of shear stress [13, 14]. In 2017, Xiao et al [15] concluded that a circular groove thickness reduction is a feasible method to reach larger deformation in the central area and weaken stress concentration at the fillet between the arms. Nevertheless, the shape and position of fillet between adjacent arms also have great influence on the experimental result. As Hu et al [16] pointed out that a cruciform with a cut-in fillet not only shows higher strain uniformity in the central region, but also enables to raise the strain level. In this study, aiming to further optimize the position of fillet, various simulations with different shape of specimen were performed by using finite element code ABAQUS/Explicit. The dimensions of the geometry shape are illustrated as figure 4. Point P denotes the central position of fillet, which could be indirectly expressed by the distances from Point P to the symmetrical axes in horizontal and vertical directions (marked as D in the figure). The finite element model was established, as shown in figure 5. The material property was assigned from the experimental results. The central zone was meshed with the size of 0.2mm in order to observe the deformation more accurately, while four straight arms were meshed by 2mm mesh for the consideration of computational efficiency. The anisotropic yield behaviour was described by Yld2000-2d yield criterion and the parameters were listed in table 4.

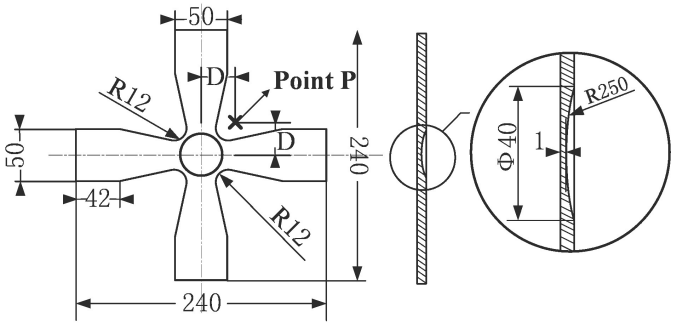


Figure 4. Dimension of specimen(unit:mm).

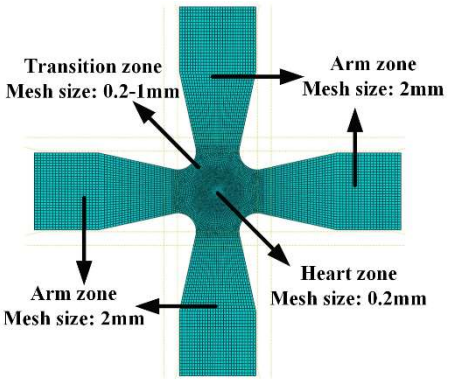


Figure 5. The finite element model of cruciform specimen.

As ranging D from 23 to 31 (labelled as $D_i (i = 23, 25, 27, 29, 31)$ for convenience) with the incremental step length of 2, various simulations were performed under the equi-biaxial tension state. The strain in the central area of the specimen along with time were checked and plotted in figure 6. As can be seen from the figure, the specimen with different D_i could reach the same strain level, which

was sufficient to characterize the forming limit of the AA5000 series aluminium alloys [17]. However, to achieve the same deformation in the central zone, the greater D_i is adopted, the longer time is required. As a result, reducing D_i could effectively shorten the test procedures. To avoid premature arm fracture during the experiments, the evolution of Mises stress with time at the fillet between two perpendicular arms were observed and shown in figure 7. As depicted in the figure, the curve of D_{23} presented obviously higher than the others, which indicated that more stress was concentrated in the corner and could result in the premature fracture of arms. In conclusion, the specimen with D_{25} seems to be more effective.

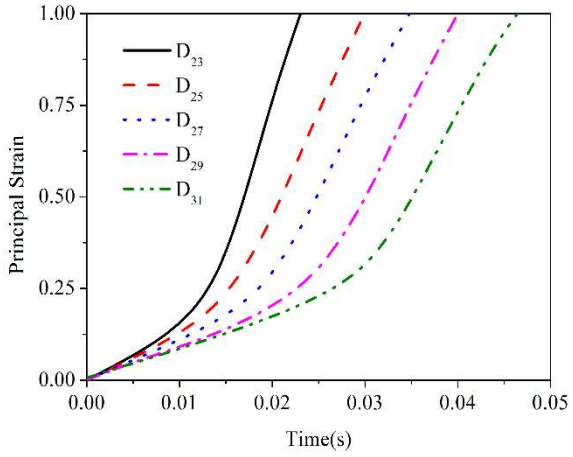


Figure 6. The principal strain-time curves at central zone.

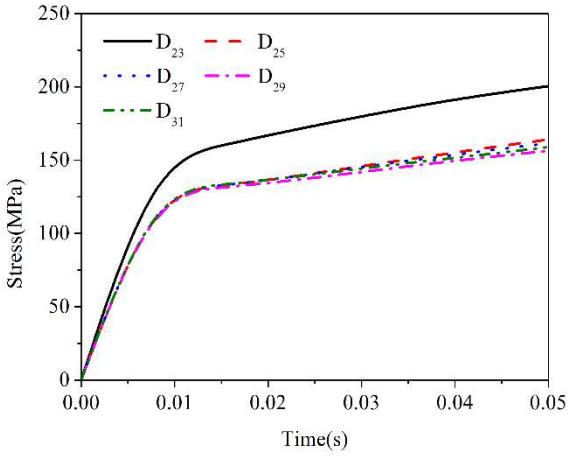
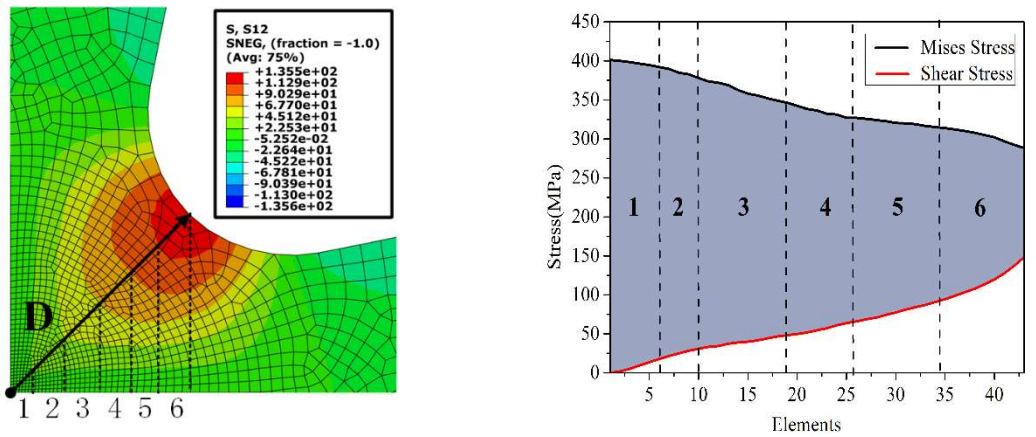


Figure 7. The Mises stress- time curves at the fillet.

The shear stress distribution of specimen with D_{25} was shown in figure 8. The shear stress was mainly concentrated upon the corners between neighbour arms. As closing to the central zone of the specimen, the shear stress was gradually decreased and became approximately zero. It is well confirmed that the effect of the shear stress can be effectively eliminated by means of the thickness reduction of specimen.



(a). The Shear stress distribution. (b). Stress distribution along D direction.

Figure 8. The Shear stress distribution and stress distribution along D direction.

4. Experiments and Results

The cruciform specimens with the discussed geometry were tested under the condition of different load ratios in order to obtain the forming limit strain at different stress states. The load ratios were as follows 4:1, 4:2, 4:3 and 4:4. The tests were recorded by a CCD camera and the image sequences were calculated by the DSCM software. The fracture zone of all employed specimens were occurred in the central region without any premature arm fracture, as shown in figure 9.

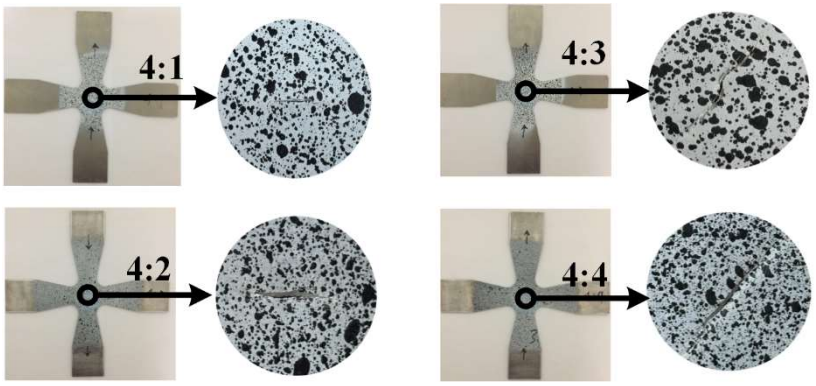


Figure 9. The specimens and its fracture zones.

In order to determine the onset of necking during the test, two points are chosen as shown in figure 10. Point B is near the fracture zone and Point A is outside the zone. The difference of strain rates between Point A and Point B throughout the test was expressed as follows [18]:

$$\delta=\frac{d\varepsilon_1^A-d\varepsilon_1^B}{dt} \tag{8}$$

Where $d\varepsilon_1^A$ and $d\varepsilon_1^B$ denote the strain rate of Point A and Point B, respectively. It could be confirmed that δ was close to 0 due to the similar deformation rate at the early stage. Nevertheless, when necking phenomenon occurred on Point A, δ would rapidly rise up. At this moment, the strain pair of Point A was extracted as the forming limit strain.

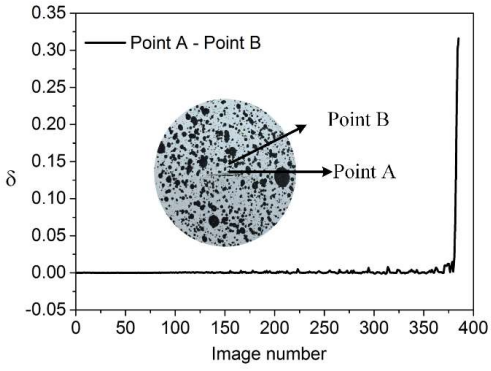


Figure 10. The central region of deformed cruciform specimen.

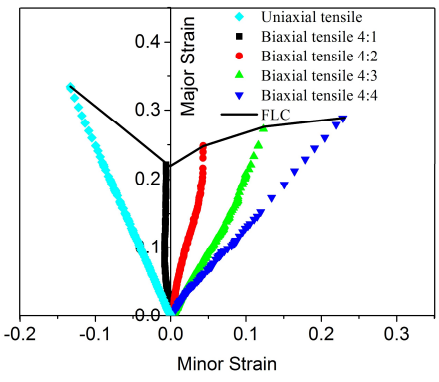


Figure 11. The forming limit curve of AA5754-O.

The strain paths of each specimen, including uniaxial and biaxial tensile tests, were presented in figure 11. The whole forming limit curve consisted of the principal forming limit strain pairs under different loading conditions. Due to the anisotropy of the sheet metal, the strain path in the central zone

of the specimen was not strictly in accordance with the balance biaxial strain state, despite of the applied equal-biaxial loading condition.

5. Conclusion

In this paper, the formability of AA5754-O was analysed based on biaxial tensile tests. Mechanical materials parameters were explored, and then the independent anisotropy parameters in Yld2000-2d yield criterion were calculated. The experimental FLC of the sheet metal was finally obtained by means of the uniaxial tensile tests and the biaxial tensile tests with the optimized cruciform specimens. Meanwhile, the feasibility of the purposed cruciform specimen was well verified.

References

[1] Handin, J. 1966. Section 10: Strength and ductility. *Geol. Soc. of America Memoirs*
[2] Groth, A., Schedin, E., and Moshfegh, R. 2014. Investigation of different techniques to evaluate the FLC from experiments and FE simulations. *Key Eng. Mater*. **611-612** 41-48
[3] Ma X, Li F, Li J, et al. Analysis of forming limits based on a new ductile damage criterion in St14 steel sheets[J]. *Materials & Design*, **2015**, 68:134-145.
[4] Marciniak Z, Kuczyński K. Limit strains in the processes of stretch-forming sheet metal [J]. Int. *J. Mech. Sci.*, 1967, **9(9):609**, IN1, 613-612, IN2, 620.
[5] Ma, B., Diao, K., Wu, X., Li, X., Wan, M., and Cai, Z. 2016. The effect of the through-thickness normal stress on sheet formability. *J. Manu. Processes* **21** 134-140
[6] Liu, B., Lang, L., Du, P., Zeng, Y., and Liu, K. 2012. RETRACTED: Effect of through thickness normal stress on forming limit at elevated temperature investigated by using modified M–K model. *Int. J. of Mater. Forming* **8** 1-18
[7] Institution, B. S. Metallic materials - sheet and strip - biaxial tensile testing method using a cruciform Test Piece.
[8] Zidane I, Guines D, Léotoing L, et al. Development of an in-plane biaxial test for forming limit curve (FLC) characterization of metallic sheets [J]. *Meas. Sci. Technol*., 2014, **21(5)**:055701.
[9] T. Kuwabara, 1.06 — biaxial stress testing methods for sheet metals, in: Y. SHFBJVT (Ed.), *Comprehensive Materials Processing*, Elsevier, Oxford 2014, pp. 95–111.
[10] Wang H, Yan Y, Han F, et al. Experimental and theoretical investigations of the forming limit of 5754O aluminum alloy sheet under different combined loading paths [J]. *Int. J. Mech. Sci.*, 2017, **133**.
[11] T. Mánik, B. Holmedal, O.S. Hopperstad, Strain-path change induced transients in flow stress, work hardening and r -values in aluminum, *Int. J. Plast*., **69** (2015) 1-20.
[12] Pan, B., Asundi, A., Xie, H., and Gao, J. 2009. Digital image correlation using iterative least squares and pointwise least squares for displacement field and strain field measurements. *Opt. Laser Eng.* **47** 865-874
[13] Y. Seymen, B. Güler, M. Efe (2016) Large Strain and Small-Scale Biaxial Testing of Sheet Metals. Exp Mech **56** 1519-1530.
[14] T. Kuwabara (2014) 1.06 – Biaxial Stress Testing Methods for Sheet Metals, *Comp Mater Process* 95-111.
[15] R. Xiao, X.X. Li, L.H. Lang, Q. Song, K.N. Liu (2017) Forming limit in thermal cruciform biaxial tensile testing of titanium alloy. *J Mater Process Tech* **240** 354-361.
[16] J. J. Hu, G. W. Chen, Y. C. Liu, and S. S. Hsu, *Exp. Mech.*, 2013, **54(4)**, 615-631.
[17] Abedrabbo N, Pourboghrat F, Carsley J. Forming of AA5182-O and AA5754-O at elevated temperatures using coupled thermo-mechanical finite element models[J]. *Int. J. Plast.*, 2007, **23(5)**:841-875.
[18] Yuan W, Wan M, Wu X. Prediction of Forming Limit Curves for 2021 Aluminum Alloy[J]. *Procedia Eng.*, 2017, **207**:544-549.